PHYSICAL REVIEW B, VOLUME 65, 161203(R)

Electronic structure of $In_{1-x}Mn_xAs$ studied by photoemission spectroscopy: Comparison with $Ga_{1-x}Mn_xAs$

J. Okabayashi, T. Mizokawa, D. D. Sarma,* and A. Fujimori
Department of Complexity Science and Engineering and Department of Physics, University of Tokyo, Bunkyou-ku, Tokyo 113-0033, Japan

T. Slupinski,† A. Oiwa, and H. Munekata‡
Kanagawa Academy of Science and Technology (KAST), 3-2-1 Sakado, Takatsu-ku, Kawasaki, 213-0012, Japan
(Received 26 November 2001; revised manuscript received 19 February 2002; published 8 April 2002)

We have investigated the electronic structure of the p-type diluted magnetic semiconductor $In_{1-x}Mn_xAs$ by photoemission spectroscopy. The Mn $3d$ partial density of states is found to be basically similar to that of $Ga_{1-x}Mn_xAs$. However, the impurity-band-like states near the top of the valence band have not been observed by angle-resolved photoemission spectroscopy unlike $Ga_{1-x}Mn_xAs$. This difference would explain the difference in transport, magnetic and optical properties of $In_{1-x}Mn_xAs$ and $Ga_{1-x}Mn_xAs$. The different electronic structures are attributed to the weaker Mn $3d$-As $4p$ hybridization in $In_{1-x}Mn_xAs$ than in $Ga_{1-x}Mn_xAs$.

DOI: 10.1103/PhysRevB.65.161203 PACS number(s): 79.60.Bm, 75.50.Pp, 75.70.Pa, 75.30.Et

Diluted magnetic semiconductors (DMS) have attracted much attention because of the combination of magnetic and semiconducting properties and hence high potential for new device applications. Recently DMS based on III-V compounds have been extensively studied because of the success in doping high concentrations of transition-metal ions by molecular beam epitaxy (MBE).[1] Most remarkably, Mn doping in InAs and GaAs leads to ferromagnetism and interesting magneto-transport properties.[2,3] This behavior is generally called "carrier-induced ferromagnetism" because hole carriers introduced into the system mediate the ferromagnetic coupling between the Mn ions[4] although its microscopic mechanism has been controversial until now. The key to clarify the mechanism of the carrier-induced ferromagnetism is to understand the nature of the doped hole carriers as well as the exchange interaction between the holes in host valence band and the localized d orbitals of the magnetic ions, so-called p-d exchange interaction. For $Ga_{1-x}Mn_xAs$, previous investigations including photoemission studies[6,7] have revealed that the basically localized Mn $3d$ electrons interact with the doped holes through the p-d hybridization which causes the p-d exchange interaction.[4]

As for the closely related system $In_{1-x}Mn_xAs$, there are several differences from $Ga_{1-x}Mn_xAs$.[4] (1) The Curie temperature is relatively low: $T_c \leqslant 55$ K.[5] (2) Optical absorption measurements have indicated that $In_{1-x}Mn_xAs$ shows a Drude-like behavior due to free carriers.[8] For $Ga_{1-x}Mn_xAs$, on the other hand, a broad peak was observed around 200 meV and there was no clear Drude component.[9] So far, no photoemission study has been reported for $In_{1-x}Mn_xAs$. Comparative studies of $Ga_{1-x}Mn_xAs$ and $In_{1-x}Mn_xAs$ would provide us with useful information to elucidate the origin of the ferromagnetism in these systems. The electronic structure of $In_{1-x}Mn_xAs$ itself is also interesting because it has been reported that $In_{1-x}Mn_xAs$ grown on GaSb substrate exhibits photo carrier-induced ferromagnetism,[10,11] and field-induced ferromagnetism.[12] Investigation of the electronic structure, especially of the hybridization and the exchange interaction between the host valence band and the localized magnetic ions, as well as the magnetic coupling between the magnetic ions, would give us a useful guideline for further development in functional materials design. Although several theoretical models have been discussed,[13–16] there are few experimental investigations to clarify the electronic structure and the mechanism of carrier-induced ferromagnetism. The purpose of this paper is to clarify the electronic structure of $In_{1-x}Mn_xAs$ by resonant photoemission spectroscopy (RPES), which yields the Mn $3d$ partial density of states (DOS), and by angle-resolved photoemission spectroscopy (ARPES), which measures the energy-band dispersions. We compare the present results with those of $Ga_{1-x}Mn_xAs$.[6,7]

A p-type $In_{1-x}Mn_xAs$/GaSb sample of 30 nm thickness was grown by MBE.[17,4] The sample had a Curie temperature of 35 K and the Mn content was estimated to be $x=0.09$ based on the calibration of beam fluxes during MBE growth. Experiments were performed at beamline BL 18-A of Photon Factory, High Energy Accelerator Research Organization, using an ADES-500 analyzer for ARPES and a CLAM-II analyzer for angle-integrated RPES. The total energy resolution was set to 100 meV, comparable to the thermal broadening at the room temperature where all experiments were carried out. The angular resolution of the ADES-500 and CLAM-II analyzers were $\pm 1°$, $\pm 4°$, respectively. To remove oxidized surface layers and other contamination, we made repeated Ar-ion sputtering (1 kV) and annealing. The annealing temperature was limited to 200°C to avoid the segregation of MnAs clusters.[18] The cleaned surface showed a 1×1 low energy electron diffraction pattern. We checked the chemical composition of the sample by measuring x-ray photoemission spectra of In, As, and Mn core levels. For angle-integrated RPES in the Mn $3p$ to $3d$ absorption region, photons of $h\nu=46-55$ eV were used. In the case of ARPES, electrons emitted in the direction normal to the surface, which come from the $\Gamma-\Delta-X$ line in the Brillouin zone, were collected. We compared the $In_{1-x}Mn_xAs$ spectra with those of the reference p-type InAs. The identical procedure of surface cleaning was performed also for the InAs sample. Binding energies are referenced to the Fermi edge of Ta spectra in electrical contact with the sample.

 ©2002 The American Physical Society

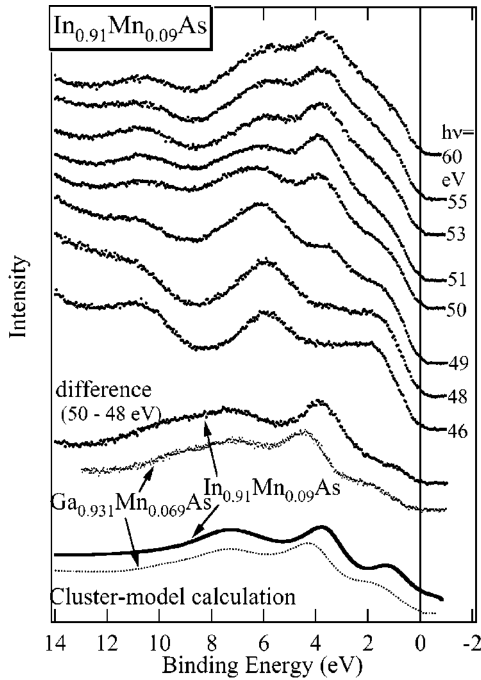

FIG. 1. A series of photoemission spectra of $In_{0.91}Mn_{0.09}As$ at various photon energies in the Mn $3p$-$3d$ core excitation threshold. The difference spectra between the on-resonant ($h\nu=50$ eV) and off-resonant (48 eV) spectra, which is a measure of the Mn $3d$ partial density of states, is shown at the bottom and is compared with configuration interaction cluster calculation results assuming the Mn^{2+} ground-state configuration. Similar comparison is shown for $Ga_{1-x}Mn_xAs$ (Ref. 6).

Figure 1 shows RPES spectra recorded using photon energies of $h\nu=46-55$ eV. The spectra have been normalized to the photon flux. Resonant enhancement occurred at $h\nu=50$ eV and off-resonance spectra were taken at $h\nu=48$ eV. The difference between the two curves yields the Mn $3d$-derived spectra as in the case of $Ga_{1-x}Mn_xAs$.[6] The difference spectrum shows a sharp peak at ~ 4 eV binding energy as well as a broad peak at ~ 7 eV binding energy. There is little intensity at the Fermi level (E_F). Such a spectral line shape is almost identical to that of $Ga_{1-x}Mn_xAs$, which has been interpreted in terms of configuration-interaction cluster-model calculations. From that analysis, the ground state has been found to be dominated by the $3d^5$ configuration.[6] These spectra also indicate strong hybridization between the Mn $3d$ electrons and the As $4p$-derived valence band.

As shown at the bottom of Fig. 1, we compare the experimental Mn $3d$ partial DOS of $In_{1-x}Mn_xAs$ with configuration-interaction cluster-model calculations. For comparison, we also show the result for $Ga_{1-x}Mn_xAs$. The parameters for the cluster-model calculations are the charge-transfer energy Δ from the ligand p level to the transition-metal d level, the on-site Coulomb energy U between two Mn $3d$ electrons, and the hybridization strength $(pd\sigma)$ between the ligand p orbital and the transition-metal d orbitals defined by Slater-Koster parameters. The details of the calculations are given in Ref. 21. The Mn $3d$-derived spectrum has been reproduced using parameters with a smaller $(pd\sigma)$ value compared to that for $Ga_{1-x}Mn_xAs$ as summarized in Table I. According to the cluster-model calculations, the ~ 2 eV feature predominantly consists of $d^5\underline{L}$ final states, while the satellite structure comes from the d^4 final-state configuration because $E(d^4)-E(d^5\underline{L})\sim U-\Delta>0$. Using the above parameters, we have estimated the p-d exchange interaction in $In_{1-x}Mn_xAs$ to be $N\beta=-0.7$ eV. This value is smaller than that of $Ga_{1-x}Mn_xAs$ ($N\beta=-1.0$ eV).[6] The depressed intensity at E_F in the difference spectrum compared to the valence-band intensity at E_F for various photon energies both for $In_{1-x}Mn_xAs$ and $Ga_{1-x}Mn_xAs$ indicates that the Mn $3d$ DOS are not dominant at E_F and suggests that hole carriers of As $4p$ character contribute to the transport.

TABLE I. Electronic structure parameters Δ, U, and $(pd\sigma)$ and the exchange coupling constant $N\beta$ for substitutional Mn impurities in InAs and GaAs in units of eV. Error bars from the line-shape analyses are ± 0.5 eV for Δ and U, and ± 0.1 eV for $(pd\sigma)$.

Material	Δ	U	$(pd\sigma)$	$N\beta$	
$Ga_{1-x}Mn_xAs$	1.5	3.5	−1.0	−1.0	Ref. 6
$In_{1-x}Mn_xAs$	1.0	3.5	−0.8	−0.7	This work

The difference spectrum between $In_{1-x}Mn_xAs$ and pure InAs taken at $h\nu=70$ eV has also been used to obtain the Mn $3d$ partial DOS as shown in Fig. 2. The spectra have been normalized to the In $4d$ core-level peaks taking into account the composition difference between In and Mn. Because of the Cooper minimum of the As $4p$ states at $h\nu \sim 70$ eV, the ionization cross section of As $4p$ reaches a minimum, and the Mn $3d$ component is relatively enhanced.[22] The line shape of the difference spectrum is almost the same as that in Fig. 1, which guarantees that the Mn $3d$ density of states deduced from RPES is valid to discuss the electronic structure.

To obtain more information about the electronic structure around E_F, we have measured ARPES spectra along the $\Gamma-\Delta-X$ line for both $In_{1-x}Mn_xAs$ and InAs. As shown in Fig. 3, by changing the photon energy in the normal emission set up from the (001) surface,[23] the energy band dispersions along the $\Gamma-\Delta-X$ line were observed. According to the direct-transition model for ARPES with an appropriate inner potential (10 eV),[24] the Γ point is measured at $h\nu\sim 10$ eV and the X point is measured at $h\nu\sim 32$ eV. The peaks in Fig. 3(a) correspond to the Δ_1 band (split-off band) and $\Delta_3+\Delta_4$ band (heavy- and light-hole bands, respectively) along the $\Gamma-\Delta-X$ line. The clear dispersion curves are almost the same as those for GaAs and InAs. Due to the Mn $3p$-$3d$ resonant effect, the line shape changes drastically around $h\nu=50$ eV, almost in the same way as in the RPES result. Comparison of the spectra near E_F between $In_{1-x}Mn_xAs$ and InAs shown in Fig. 3(b) reveals no clear differences in spite of Mn doping. This is quite different from the case of $Ga_{1-x}Mn_xAs$ and GaAs, where impurity-band-like new states were found to form near the valence-band maximum (VBM) by Mn doping as shown in Fig. 3(c). Although Mn

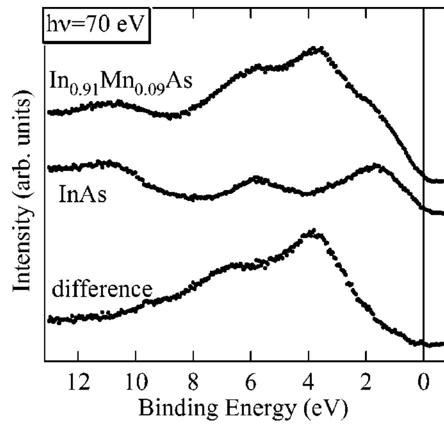

FIG. 2. Angle-integrated photoemission spectra of $In_{0.91}Mn_{0.09}As$ and InAs at $h\nu=70$ eV, where the Mn $3d$ cross section is large compared with As $4p$, and their difference spectrum representing the Mn $3d$ partial density of states.

doping in GaAs induces split-off states above the VBM through hybridization with As $4p$ and forms the impurity-band-like states, Mn in InAs does not induce such states, probably because of the weaker hybridization strength $(pd\sigma)$ than in GaAs. In fact, in the dilute limit of Mn in InAs (Mn:8×10^{16} cm^{-3}), Mn doping leads to the formation of an acceptor level of primarily As $4p$ character at 30 meV above the VBM,[19] which is much smaller than that for Mn in GaAs (100 meV).[20]

Now we discuss the origin of the differences between the electronic structure of $In_{1-x}Mn_xAs$ and $Ga_{1-x}Mn_xAs$. Comparing Mn $3d$ spectral features in $In_{1-x}Mn_xAs$ and $Ga_{1-x}Mn_xAs$, we find that the main peak in $In_{1-x}Mn_xAs$ has a lower binding energy compared to that in $Ga_{1-x}Mn_xAs$, suggesting a lower Δ in $In_{1-x}Mn_xAs$. There are two possible reasons for the decrease of the hybridization strength $(pd\sigma)$ in $In_{1-x}Mn_xAs$ compared to that in $Ga_{1-x}Mn_xAs$. One is the differences in the Mn-As distance in these two systems. Extended x-ray-absorption fine-structure measurements were performed and the Mn-As distance was reported to be 2.44 Å for $Ga_{1-x}Mn_xAs$ (Ref. 25) and 2.54–2.58 Å for $In_{1-x}Mn_xAs$.[26] The longer Mn-As distance in $In_{1-x}Mn_xAs$ would lead to a decrease in the p-d hybridization strength. Second, because of the smaller band gap in InAs (0.4 eV) than that in GaAs (1.5 eV), the In $5s$ states in the unoccupied part is more strongly mixed with the As $4p$ states in the valence band than in the case of Ga $4s$ states in GaAs. Through the mixing with the In $5s$ states, the As $4p$ weight in the valence band is reduced and hence the hybridization between the valence band and the Mn $3d$ state would decrease. Due to the weaker hybridization between the host valence band and Mn $3d$, the acceptor levels in $In_{1-x}Mn_xAs$ are not so strongly split off from the valence band maximum (VBM) and the Mn ions find it difficult to bind holes. The bound hole picture (Mn^{2+} + bound hole) is therefore less appropriate for $In_{1-x}Mn_xAs$ than for $Ga_{1-x}Mn_xAs$, and holes in $In_{1-x}Mn_xAs$ behave as free carriers. This would naturally explain the difference in the optical properties of $In_{1-x}Mn_xAs$ and $Ga_{1-x}Mn_xAs$.[8,9]

The formation of the impurity-band-like states around E_F would be important for the magneto-transport properties of the Mn doped DMS. According to the electron paramagnetic resonance (EPR) measurements, the Mn $3d$ signals of $Ga_{1-x}Mn_xAs$ (Ref. 27) showed that the Mn impurities in this system were predominantly in the ionized state (Mn^{2+},A^-). Similar picture was also obtained for n-type $In_{1-x}Mn_xAs$ (Ref. 28) in which incorporated Mn is ionized by the excess donors. From the view point of photoemission spectroscopy, the Mn $3d$ spectrum in Fig. 1 is analyzed using the cluster model with the Mn^{2+} ground state as in the case of $Ga_{1-x}Mn_xAs$. These results support that the Mn $3d$ electronic configuration is similar comparing $Ga_{1-x}Mn_xAs$ and $In_{1-x}Mn_xAs$. However, it is difficult to distinguish between the Mn^{2+} states with a weakly bound hole and with a free hole. In both $In_{1-x}Mn_xAs$ and $Ga_{1-x}Mn_xAs$, the itinerant

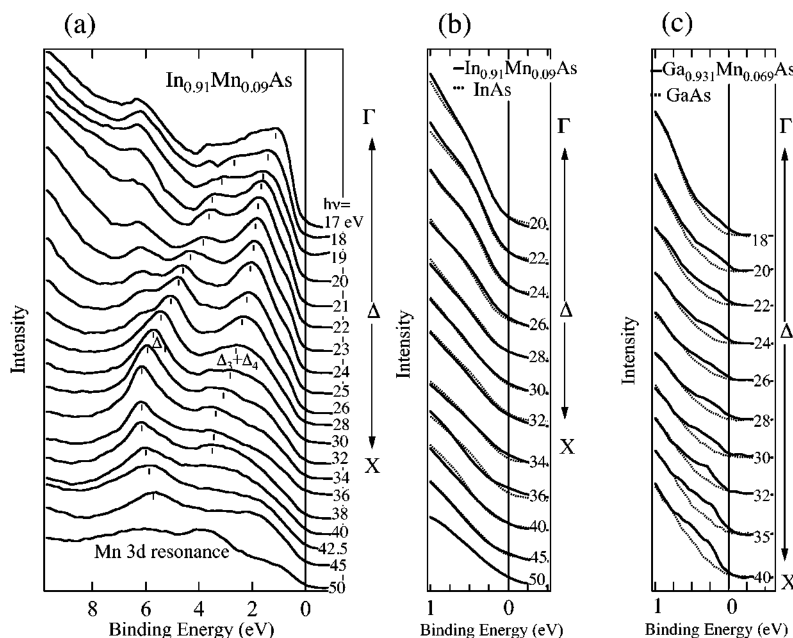

FIG. 3. Angle-resolved photoemission spectra of $In_{1-x}Mn_xAs$ along the $\Gamma-\Delta-X$ direction. (a) Wide-range spectra. Vertical bars show peak or shoulder positions. (b) Narrow-range spectra near the Fermi level for $In_{0.91}Mn_{0.09}As$ (solid curves) and InAs (dashed curves). (c) Corresponding spectra for $Ga_{1-x}Mn_xAs$ and GaAs taken from Ref. 7.

holes obviously mediate the ferromagnetic order.[4] The ferromagnetism in the double-perovskite compound Sr_2FeMoO_6 is also considered to be caused by the same mechanism as the Mn-doped DMS in the sense that the O $2p$ doped hole mediates the ferromagnetism through the gain in kinetic energy in the ferromagnetic state.[29,16] The peculiar feature in $Ga_{1-x}Mn_xAs$ is that impurity-band-like states are split off from the VBM, suggesting virtually bound holes rather than simple free carriers of $In_{1-x}Mn_xAs$. The formation of these states may help to increase the T_c of $Ga_{1-x}Mn_xAs$ compared to $In_{1-x}Mn_xAs$ but more studies are necessary to clarify the mechanism for this.

In conclusion, we have investigated the electronic structure of $In_{1-x}Mn_xAs$ using ARPES and RPES and compared it with $Ga_{1-x}Mn_xAs$. Although the Mn $3d$ states are in the Mn^{2+} configuration in both systems, impurity-band-like states are not observed in $In_{1-x}Mn_xAs$ unlike $Ga_{1-x}Mn_xAs$. We attribute this to the weaker hybridization in $In_{1-x}Mn_xAs$ than in $Ga_{1-x}Mn_xAs$, that is not sufficient to split off states from the VBM to form the impurity-band-like states.

This work was performed under the approval of the Photon Factory Program Advisory Committee (Proposal No. 99G140). J.O. acknowledges support from the Japan Society for the Promotion of Science for Young Scientists.

---

*Permanent address: Solid State and Structural Chemistry Unit, Indian Institute of Science, Bangalore 560 012, India.

†Present address: Institute of Experimental Physics, Warsaw University, Hoza 69, 00-681 Warsaw, Poland.

‡Original post at: Imaging Science and Engineering Laboratory, Tokyo Institute of Technology, Nagatsuda, Midori-ku, Yokohama 226-8503, Japan.

[1] H. Munekata, H. Ohno, S. von Molnar, A. Segmuller, and L.L. Chang, Phys. Rev. Lett. **63**, 1849 (1989).

[2] H. Ohno, Science **281**, 951 (1998).

[3] A. Oiwa, A. Endo, S. Katsumoto, Y. Iye, H. Ohno, and H. Munekata, Phys. Rev. B **59**, 5826 (1999); Y. Iye, A. Oiwa, A. Endo, S. Katsumoto, F. Matsukura, A. Shen, H. Ohno, and H. Munekata, Mater. Sci. Eng. B **63**, 88 (1999).

[4] H. Ohno, J. Magn. Magn. Mater. **200**, 110 (2000).

[5] T. Slupinski, A. Oiwa, and H. Munekata, J. Cryst. Growth **237–239**, 422 (2002).

[6] J. Okabayashi, A. Kimura, T. Mizokawa, A. Fujimori, T. Hayashi, and M. Tanaka, Phys. Rev. B **59**, R2486 (1999).

[7] J. Okabayashi, A. Kimura, O. Rader, T. Mizokawa, A. Fujimori, T. Hayashi, and M. Tanaka, Phys. Rev. B **64**, 125304 (2001).

[8] K. Hirakawa, A. Oiwa, and H. Munekata, Physica E **10**, 215 (2001).

[9] K. Hirakawa, Y. Hashimoto, T. Hayashi, S. Katsumoto, and Y. Iye, Phys. Rev. B (to be published).

[10] S. Koshikara, A. Oiwa, M. Hirasawa, S. Katsumoto, Y. Iye, C. Urano, H. Takagi, and H. Munekata, Phys. Rev. Lett. **78**, 4617 (1997).

[11] A. Oiwa, T. Slupinski, and H. Munekata, Appl. Phys. Lett. **78**, 518 (2001).

[12] H. Ohno, D. Chiba, F. Matsukura, T. Omiya, E. Abe, T. Dietl, Y. Ohno, and K. Ohtani, Nature (London) **408**, 944 (2000).

[13] H. Akai, Phys. Rev. Lett. **81**, 3002 (1998).

[14] J. Inoue, S. Tonoyama, and H. Itoh, Phys. Rev. Lett. **85**, 4610 (2000).

[15] T. Dietl, H. Ohno, F. Matsukura, J. Cibert, and D. Ferrand, Science **287**, 1019 (2000).

[16] J. Kanamori, and K. Terakura, J. Phys. Soc. Jpn. **70**, 1433 (2001).

[17] H. Munekata, A. Zaslavsky, P. Fumagalli, and R.J. Gambino, Appl. Phys. Lett. **63**, 2929 (1993).

[18] Y. Hashimoto, T. Hayashi, S. Katsumoto, and Y. Iye, J. Cryst. Growth (to be published).

[19] E.I. Georgitse, I.T. Postolaki, V.A. Smirnov, and P.G. Untila, Sov. Phys. Semicond. **23(4)**, 469 (1989).

[20] M. Linnarsson, E. Janzen, B. Monemar, M. Kleverman, and Thilderkvist, Phys. Rev. B **55**, 6938 (1997).

[21] T. Mizokawa and A. Fujimori, Phys. Rev. B **48**, 14 150 (1993).

[22] J.-J. Yeh and I. Lindau, At. Data Nucl. Data Tables **32**, 1 (1985).

[23] S. Hüfner, *Photoelectron Spectroscopy* (Springer-Verlag, Berlin, 1995).

[24] T.C. Chiang, J.A. Knapp, M. Aono, and D.E. Eastman, Phys. Rev. B **21**, 3513 (1980).

[25] R. Shioda, K. Ando, T. Hayashi, and M. Tanaka, Phys. Rev. B **58**, 1100 (1998).

[26] Y.L. Soo, S.W. Huang, Z.H. Ming, T.H. Kao, H. Munekata, and L.L. Chang, Phys. Rev. B **53**, 4905 (1996).

[27] J. Szczytko, A. Twadowski, K. Swiatek, M. Palczewska, T. Hayashi, M. Tanaka, and K. Ando, Phys. Rev. B **60**, 8304 (1999).

[28] J. Szczytko, A. Twadowski, M. Palczewska, R. Jalonski, J. Furdyna, and H. Munekata, Phys. Rev. B **63**, 085315 (2001).

[29] D.D. Sarma, P. Mahadevan, T.S. Dasgupta, S. Ray, and A. Kumar, Phys. Rev. Lett. **85**, 2549 (2000); D.D. Sarma, Curr. Opin. Solid State Mater. Sci. **5**, 261 (2001).